ORIGINAL ARTICLE

# A New Method for Measuring the Oxygen Diffusion Constant and Oxygen Consumption Rate of Arteriolar Walls

**Nobuhiko Sasaki,[1] Hirohisa Horinouchi,[3] Akira Ushiyama [2] and Haruyuki Minamitani [1]**

*[1] Graduate School of Science and Technology, Keio University, Tokyo, Japan*
*[2] Department of Environmental Health, National Institute of Public Health, Saitama, Japan*
*[3] Department of Surgery, School of Medicine, Keio University, Tokyo, Japan*

(Received for publication on March 29, 2011)
(Revised for publication on July 6, 2011)
(Accepted for publication on July 27, 2011)

**Oxygen transport is believed to primarily occur via capillaries and depends on the oxygen tension gradient between the vessels and tissues. As blood flows along branching arterioles, the $O_2$ saturation drops, indicating either consumption or diffusion. The blood flow rate, the $O_2$ concentration gradient, and Krogh's $O_2$ diffusion constant (*K*) of the vessel wall are parameters affecting $O_2$ delivery. We devised a method for evaluating *K* of arteriolar wall *in vivo* using phosphorescence quenching microscopy to measure the partial pressure of oxygen in two areas almost simultaneously. The *K* value of arteriolar wall (inner diameter, 63.5 ± 11.9 μm; wall thickness, 18.0 ± 1.2 μm) was found to be $6.0 \pm 1.2 \times 10^{-11}$ ($cm^2/s$)(ml $O_2 \cdot cm^{-3}$ tissue$\cdot mmHg^{-1}$). The arteriolar wall $O_2$ consumption rate (*M*) was 1.5 ± 0.1 (ml $O_2 \cdot 100\ cm^{-3}$ tissue$\cdot min^{-1}$), as calculated using Krogh's diffusion equation. These results suggest that the arteriolar wall consumes a considerable proportion of the $O_2$ that diffuses through it.** (Keio J Med 61 (2) : 57–65, June 2012)

***Keywords*: oxygen transportation, microcirculation, Krogh's cylinder model, phosphorescence quenching method**

## Introduction

Oxygen transport occurs by diffusion and is driven by a concentration gradient. Krogh presented a cylinder model to explain oxygen diffusion.[1,2] In Krogh's model, oxygen is believed to be supplied to tissues by capillaries. However, the oxygen saturation of hemoglobin in arteriolar blood decreases with increasing arteriolar branching.[3] Several studies have reported that oxygen diffuses through arterioles to tissues.[4–6] Clarifying the oxygen diffusion constant and consumption rate should improve our understanding of this phenomenon. To elucidate oxygen consumption by, and diffusion through, arterioles, Krogh's oxygen diffusion constant (*K*) of the arteriolar wall and the oxygen consumption rate (*M*) of the arteriolar wall must be determined; *K* is the product of the diffusion constant of oxygen (*D*) and oxygen solubility ($\alpha$).[2] Recently, the drop in the partial pressure of oxygen ($pO_2$) across the blood–tissue interface[6] and the drop in $pO_2$ in the arteriolar wall[7] were reported to be greater than those in the tissue outside the arteriole. These observations indicate that either *K* of the arteriolar wall is extremely low or that *M* of the arteriolar wall is extremely high.[6] We therefore sought to produce an optical measurement system to evaluate *K* and *M* of the arteriolar wall *in vivo*.

The arteriolar wall consists of endothelial cells, a basement membrane, vascular smooth muscle cells, mural cells, and an interstitial matrix.[8] For an arteriole with an inner diameter of approximately 50 μm, the arteriolar wall thickness is approximately 10–20 μm.[7,9] Quantitative assessment necessitates that *K* and *M* of an arteriolar wall be measured in *vivo* without vessel damage. Using a special microscope system to precisely measure $pO_2$, we were able to calculate the values of *K* and *M* using the

Reprint requests to: Hirohisa Horinouchi MD, PhD, Department of Surgery, School of Medicine, Keio University, Shinanomachi 35, Shinjuku, Tokyo 160-8582, Japan, E-mail: horinouc@a8.keio.jp, Secondary E-mail: horinouc@sc.itc.keio.ac.jp

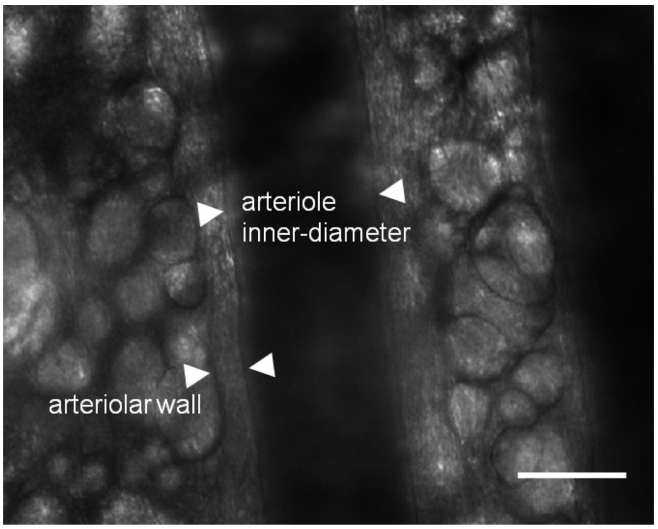


**Fig. 1** Arteriolar wall in a mouse dorsal skinfold chamber. The arteriolar wall was clearly observed under white light. The inner diameter of this arteriole was 58.4 μm and the wall thickness was 18.6 μm. The scale bar indicates 50 μm.

equations presented in earlier reports.[10–12]

## Materials and Methods

### *Animals*

Experiments were performed using the mouse dorsal skinfold chamber (DSC) model[13] on 7- to 10-week-old male BALB/c mice (Oriental Yeast, Tokyo, Japan) weighing 27–30 g. The mice were kept on a bed of pulp paper in a ventilated, temperature-controlled (23°C ±1°C), specific pathogen-free environment with a 12-h light–dark cycle. They were given access to food and water *ad libitum*. All experimental protocols were reviewed by the Committee on the Ethics of Animal Experiments at our university and were conducted in accordance with the Guidelines for Animal Experiments issued by the Keio University School of Medicine Experimental Animal Center, and Law (No. 105) and Notification (No. 6) issued by the Japanese Government. The ethical guidelines conformed to The American Physiological Society (APS) guiding principles for the care and use of animals.

Mice were anesthetized for 1 h using ketamine (90 mg/kg body weight) and xylazine (10 mg/kg body weight) for DSC implantation. Detailed procedures of implantation were described in an earlier report.[13] When the DSC was in place on the back of mice, the fascia was removed to observe the subfascial microcirculation. Each mouse was rested for at least 2 days to achieve stabilization of the microcirculation under DSC, consequently, all experiments were conducted 2–6 days after DSC implantation.

At the time of measurement, ketamine–xylazine (7–60 mg/kg body weight) was used for anesthesia induction. Sevoflurane (1%) was administered through a mask for maintenance of anesthesia. Animals were placed on a piezo stage, and the DSC was fixed with double-sided tape. The surface temperature was monitored using a thermocouple thermometer (AD5652; A&D, Tokyo, Japan).

### *Arteriolar wall*

The arteriolar wall thickness[5,7,9,14] was 10–25 μm for vessels with an inner diameter of 40–80 μm (**Fig. 1**; 27°C ±1°C tissue surface temperature in DSC; 400–500 μm tissue thickness in DSC). All arteriolar walls were observed using the transmitted light of a halogen lamp (KTS-150RSV; Kenko, Tokyo, Japan) because the excitation band of the oxygen measurement probe causes tissue photodamage. Photodamage caused by the influence of blue and green light was reduced using a wide-spectrum halogen light for a short period. The wall thickness was measured using a cooled CCD camera (DS-Qi1Mc; Nikon, Tokyo, Japan) mounted on a microscope system that was assembled specifically for use in this study (**Fig. 1**; Newopto, Yokohama, Japan; The Optronics [Sankei], Tokyo, Japan). The arteriole targeted in this study had a wall thickness of approximately 18 μm, and this accommodated the diameter of the laser beam (23 μm).

### *Probes*

Fluorescein-labeled dextran (FITC-dextran; MW 2000 kDa, 10 mg/ml, 3 mL/kg body weight; Sigma-Aldrich, St. Louis, MO, USA) was injected into the tail veins of mice to observe the microcirculation and to measure the red blood cell (RBC) velocity in arterioles. After injecting FITC-dextran, Pd-meso-tetra (4-carboxyphenyl) porphyrin (Pd-TCPP; 8.5 mg/ml, 3 mL/kg body weight; Frontier Scientific, Logan, UT, USA) was injected as an oxygen probe. The Pd-TCPP was dissolved using a mixture (8:2) of 7.5% bovine serum albumin (Life Technologies, Carisbad, CA, USA) and phosphate buffer (pH 7.4; Life Technologies, Carisbad, CA, USA). We measured $pO_2$ from 30–40 min after injecting Pd-TCPP,[15] because Pd-TCPP requires some time to spread from the vessels to the tissues. During the waiting period, animals were kept in a dark cage.

### *Microscope system for $pO_2$ measurement*

Pd-TCPP was excited by the second harmonic of a Q-switched neodymium-doped yttrium aluminium garnet pulse laser (wavelength, 532 nm; pulse width at half maximum, 6 ns; irradiation energy, 200 nJ/pulse) through the objective lens (Fluor 40×/0.80 W; Nikon) of the mi-

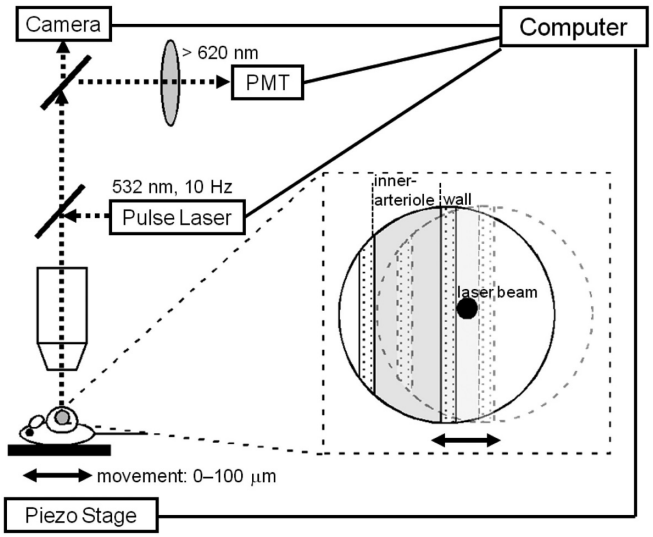


**Fig. 2** Measurement system to determine *K* of the arteriolar wall. The piezo-driven stage was used to measure $pO_2$ in two areas using a microscope. The two measurement areas were located alternately under the laser beam using the piezo stage. We simultaneously measured $pO_2$ in the two areas using Pd-TCPP and a microscope. Laser parameters: 23-μm laser spot size, 200 nJ, 10 Hz, 6-ns half bandwidth. PMT, photomultiplier tube.

croscope (**Fig. 2**).[16] The laser pulse recurrence frequency was 10 Hz (when the oxygen diffusion constant was measured) or 2 Hz (when the oxygen consumption rate and other parameters were measured). The laser beam diameter at the focus position was 23 μm. At points other than the focus position, the laser beam had a larger diameter. Phosphorescence was weak in areas other than the focus position. The photomultiplier tube (PMT; R1894; Hamamatsu Photonics, Hamamatsu, Japan) was unable to detect the weak phosphorescence at points other than the focus position. The reflected laser light and Pd-TCPP phosphorescence light were discriminated using a dichroic mirror (DM575; Nikon) and a long-pass filter (RG620; Nikon). The phosphorescence intensity signal was transformed to a current signal by the PMT. Then, the current from the PMT was transformed to a voltage signal by an analog-to-digital converter (ADC; NR-2000; Keyence, Osaka, Japan). The voltage signal from the ADC was sampled (sampling frequency, 200 kHz; 500 points sampled) using a personal computer (**Fig. 2**). Residual reflected laser light, light leaked from the laser source, and tissue autofluorescence interfered with accurate measurement of the phosphorescence signal. To eliminate these unwanted effects, the phosphorescence signal was analyzed 50 μs after initial detection of light signals.[16] The phosphorescence lifetime ($\tau$) was determined as the decay time to 1/e of the maximum phosphorescence intensity because the phosphorescence signal–intensity plot followed a single exponential curve.[16] Furthermore, $pO_2$ was calculated by measuring $\tau$ according to the Stern–Volmer equation:[5]

$$\frac{I_0}{I} = \frac{\tau_0}{\tau} = 1 + \tau_0 k_q [C] \quad (1)$$

where $C$ represents $pO_2$, $I$ is the light intensity, $I_0$ is the initial light intensity, $\tau$ is the phosphorescence lifetime, $\tau_0$ is the phosphorescence lifetime at 0 mmHg $O_2$, and $k_q$ is the quenching coefficient (0.205 $mmHg^{-1} \cdot s^{-1}$); $\tau_0$ was 0.658 ms (26.5°C) in our study following calibration.[17]

We constructed the microscope system to repeatedly observe $pO_2$ at two points almost simultaneously using a piezo-driven stage (P517.2CL; ±5 nm repeatability, 250 Hz resonance frequency at 500 g loaded; PI Japan, Tokyo, Japan) and a controller (**Figs. 2** and **3A**; E-665 CR; PI Japan). The stage vibrated horizontally within a designated distance, and motion was controlled by a personal computer (Epson Direct Model 1127113; Epson Direct, Nagano, Japan).

### *Measurement model for K*

The following assumptions were used to calculate *K* of the arteriolar wall (**Fig. 3A**):

1. When mice inhaled pure oxygen, the increase in the $pO_2$ of peri-arteriolar wall tissues was assumed to represent the increase in oxygen provided through the arteriolar wall alone, which resulted from the increase in intra-arteriolar $pO_2$.
2. Over a short period, the *M* values of the tissue and arteriolar wall were assumed to remain the same when pure oxygen was inhaled.
3. The *K* values of blood (intra-arteriolar) and peri-arteriolar tissue were assumed to be higher than that of the arteriolar wall.
4. We chose a short longitudinal segment of the arteriole to reflect our assumption that oxygen diffusion occurs in two dimensions in this model.

Following these assumptions, Krogh's oxygen diffusion constant (*K*), the oxygen diffusion constant (*D*), and the oxygen solubility of the arteriolar wall ($\alpha$) were calculated using the following equations:[2–4,10–12,18–21]

$$K = D\alpha_t \quad (2)$$

$$D = \frac{(R_c + x)^2 - R_c^2}{4t} \quad (3)$$

$$\alpha_t = \frac{\Delta P_{out}(R_c + x)}{V_t \Delta P_{in} R_c} \quad (4)$$

where $D$ is the diffusion constant of oxygen through the arteriolar wall, $\alpha_t$ is the oxygen solubility of the arteriolar

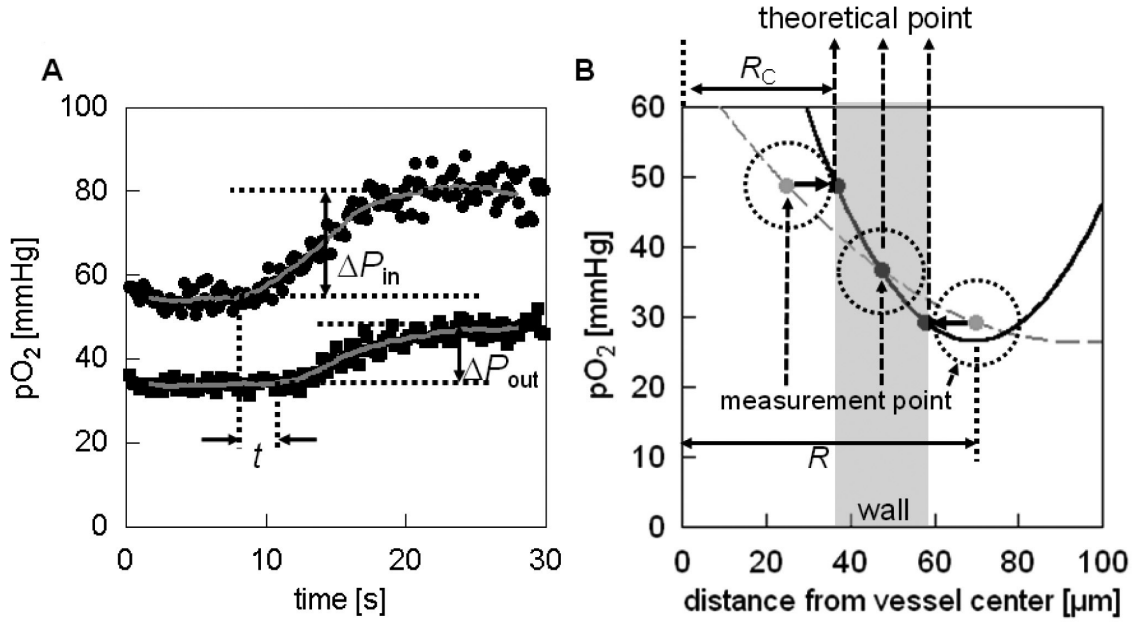


**Fig. 3** Measurements required to calculate *K* and *M* of arteriolar wall.
(A) Changes in oxygen tension were required to calculate K. This representative curve shows the simultaneous changes in $pO_2$ at intra-arteriolar and peri-arteriolar locations before and after the mouse inhaled pure oxygen. Laser shots (10-Hz excitation) were emitted from a Q-switch laser oscillator: 50% of the shots were aimed at the intra-arteriolar spot near the wall and 50% were aimed at the outer arteriolar peri-arteriolar spot. The piezo-driven stage moved back and forth with a frequency of 10 Hz. In this representative schema, the arteriole has a wall thickness and inner vessel diameter of 13.5 mm and 73.1 mm, respectively. Circle plots show intra-arteriolar $pO_2$ and square plots show outer peri-arteriolar $pO_2$. Gray lines show moving averages of intra-arteriolar and extra-arteriolar $pO_2$. It took 5 s to observe an increase in intra-arteriolar $pO_2$ after the mouse was switched to inhaling pure oxygen.
(B) Measurements of the oxygen consumption rate. The arteriole had a wall thickness and inner vessel diameter of 21.2 μm and 73.4 μm, respectively. The gray plot shows the $pO_2$ at the laser-irradiated intra-arteriolar, wall center, and peri-arteriolar areas, representative of the $pO_2$ of the inner edge, wall center, and outer edge of the arteriolar wall, respectively (black plot). The analysis given in the text explains why the theoretical fitted line is the solid line and not the dashed line. R is defined as the point of zero oxygen gradient. The gray zone represents the arteriolar wall.

wall, Rc is the inner radius of arteriole, $x$ is the thickness of the arteriolar wall, and $t$ is the oxygen diffusion time from the intra-arteriolar space to the exterior peri-arteriolar wall. In addition, $\Delta P_{in}$ is the change in $pO_2$ at the inner edge of the arteriolar blood flow, and $\Delta P_{out}$ is the change in oxygen volume at the peri-arteriolar wall. This volume change was derived from the change in $pO_2$ at the inner edge of the arteriolar blood flow when the animals were switched to inhale pure oxygen after breating normal room air, and the change in oxygen volume was transformed from the change in $pO_2$ at the exterior peri-arteriolar wall using the published oxygen solubility value for water (at 27°C and 1 atm).[22] In addition, $V_t$ is the arteriolar wall volume and $R_c$ is the inner radius of the arteriole. On the basis of Brownian motion,[20] Eq. 3 was derived from two-dimensional diffusion and molecular diffusion.[19,23] The relation between arteriolar oxygen solubility[10,11] and oxygen tension at the peri-arteriolar area and the inner-edge of the arteriolar wall are shown in Eq. 4. In the equation, $(R_c + x)/R_c$, is a factor that adjusts $\Delta P_{out}$, which might show a lower volume attributable to two-dimensional diffusion.

### *Oxygen consumption rate model*

The oxygen consumption rate of the arteriolar wall was calculated from the observed value of the arteriolar wall *K*, following the diffusion equations (Eqs. 5–8), as derived from Krogh's cylinder model.[1,2,24] In Krogh's cylinder model, the cylinder comprises one capillary and the theoretical cylinder tissue around the capillary outside the vessel wall. The cylinder tissue has an oxygen concentration gradient that is dependent on the distance from the capillary wall. At the radius of the theoretical

**Table 1.** Parameters of the arteriole

| Parameter | Value | |
|---|---|---|
| Mean red blood cell velocity | 1.75 ± 0.81 | mm/s |
| Arteriolar radius | 31.8 ± 5.9 | μm |
| Arteriolar wall thickness | 18.0 ± 1.2 | μm |
| Oxygen solubility of water (*a*) | 0.028 * | ml $O_2$/ $cm^3$ at 27°C, 760 mmHg |
| Difference of $pO_2$ between intra- and peri-arteriolar regions | 13.3 ± 2.6 | mmHg |
| Intra-arteriolar $pO_2$ | 43.2 ± 6.5 | mmHg |
| Oxygen diffusion constant of arteriolar wall (*D*) | $2.0 \pm 0.5 \times 10^{-6}$ | $cm^2$ / s |
| Oxygen solubility of the arteriolar wall ($a_t$) | $3.1 \pm 0.5 \times 10^{-5}$ | ml $O_2$ • $cm^{-3}$ tissue • $mmHg^{-1}$ |
| Krogh's $O_2$ diffusion constant of arteriolar wall (*K*) | $6.0 \pm 1.2 \times 10^{-11}$ | ($cm^2$/s)(ml $O_2$ • $cm^{-3}$ tissue • $mmHg^{-1}$) |
| Arteriolar wall $O_2$ consumption rate (*M*) | 1.5 ± 0.1 | (ml $O_2$ • 100 $cm^{-3}$ tissue • $min^{-1}$) |

Values are mean ±SE.
*Ogi and Maruzen Co., Ltd., 2010 [16].

cylinder tissue, the oxygen concentration gradient is zero. We regarded the arteriolar wall itself as comprising the cylinder tissue of Krogh's model. We defined the boundary condition of the measured values of the intra-arteriole, wall center, and peri-arteriole. The $pO_2$ value, as retrieved from the spot where the laser beam contacted the inner arteriolar wall, was assumed to be the $pO_2$ of the inner edge of the arteriole ($r = R_c$). For the $pO_2$ retrieved from the wall center spot, the value was assumed as the $pO_2$ of the wall center ($r = R_c + x/2$). The $pO_2$ retrieved from the spot where the laser beam contacted the outer arteriolar wall was assumed to be the $pO_2$ of the peri-arteriolar tissue ($r = R_c + x$) (**Fig. 3B**). The theoretical cylinder tissue radius (*R*) of the arteriolar wall was calculated as the point where $\partial P_t/\partial r = 0$ from curve fitting the oxygen diffusion gradient of the arteriolar wall (**Fig. 3B**).

$$\alpha_t \frac{\partial P_t}{\partial t} = K\left[\frac{1}{r}\frac{\partial}{\partial r} r \frac{\partial P_t}{\partial r} + \partial \frac{\partial P_t}{\partial z^2}\right] - M \quad (5)$$

$$P_t = P_w \quad at \quad r = R_c \quad (6)$$

$$\frac{\partial P_t}{\partial r} = 0 \quad at \quad r = R \quad (7)$$

$$P_t = P_w(z) + \frac{M}{4K}\left(r^2 - R_c^2\right) - \frac{MR^2}{2K}\ln\frac{r}{R_c} \quad (8)$$

where $P_t$ is the tissue $pO_2$ (mmHg), $P_w$ is the vessel wall $pO_2$ (mmHg), *r* is the distance from the vessel center, $R_c$ is the vessel radius, *K* is the oxygen diffusion constant in units of ($cm^2$/s)(ml $O_2$·$cm^{-3}$ tissue·$mmHg^{-1}$), *M* is the oxygen consumption rate in units of (ml $O_2$·$cm^{-3}$ tissue·$s^{-1}$), $\alpha_t$ is the oxygen solubility of the arteriolar wall (ml $O_2$·$cm^{-3}$ tissue·$mmHg^{-1}$), and *R* represents the cylinder tissue radius.

## Results

### *Krogh's oxygen diffusion constant of the arteriolar wall*

We used seven mice for the experiments, and measurements were taken at three locations (i.e., within the arteriolar lumen close to the wall, the arteriolar wall, and in the tissue just outside the arteriole) in the DSC for each mouse. The *K* value of the arteriolar wall was calculated from Eqs. 2–4. Parameters *t*, $\Delta P_{in}$, and $\Delta P_{out}$ were measured. A representative experimental curve is shown in **Fig. 3A**. The calculated *K* value of the arteriolar wall was $6.0 \pm 1.2 \times 10^{-11}$ ($cm^2$/s)(ml $O_2$·$cm^{-3}$ tissue·$mmHg^{-1}$) ($N = 7$), which is only around one-tenth of the *K* value for muscle described in previous reports (**Table 1, 2**). It took about 5 s to observe an increase in intra-arteriolar $pO_2$ after the mouse inhaled pure oxygen; it took another 2.0 ± 0.3 s before an increase in peri-arteriolar $pO_2$ was detected. This time difference (2.0 ± 0.3 s) was defined as the diffusion time (*t*). The $pO_2$ in each region reached a steady state after 10–20 s from the start of the increase of blood $pO_2$. The thickness of the arteriolar wall (*x*) was measured using a cooled CCD camera.

### *Oxygen consumption rate of the arteriolar wall*

The data shown in **Figure 3B** gave a calculated *M* value for the arteriolar wall of 1.5 ± 0.1 (ml $O_2$·100 $cm^{-3}$ tissue·$min^{-1}$) ($N = 7$), which is similar to the *M* values of muscles described in previous reports (**Table 2**). **Table 1** presents the arteriole parameters used in this experiment.

**Table 2.** Comparison of our results with published data

| Author/year | Animal | Area (targeted tissue) | $K^*$ ($cm^2/s$)(ml $O_2$ $\cdot cm^{-3}$ tissue $\cdot mmHg^{-1}$) | $M^{**}$ (ml $O_2 \cdot 100\ cm^{-3}$ tissue$\cdot min^{-1}$) | Method |
|---|---|---|---|---|---|
| Bentley, 1993 | Hamster | Retractor muscle (at rest, in vivo) | $9.38 \times 10^{-10}$ | 1.93 | Polarography |
| Buerk, 1982 | Rabbit | Abdominal aorta, in vivo | | 0.78 | Polarography |
| | | Thoracic aorta, in vivo | | 0.588 | Polarography |
| | Dog | Thoracic aorta, in vivo | | 0.9 | Polarography |
| Howard, 1966 | Hamster | Arteriole with anesthesia, ex vivo | | 1.44 | Cartesian diver method |
| | | Arteriole without anesthesia, ex vivo | | 1.21 | Cartesian diver method |
| | Human | Mesentery with anesthesia, ex vivo | | 0.53 | Cartesian diver method |
| Navari, 1979 | Cat | Pial artery, ex vivo | | 0.72 | Cartesian diver method |
| Paul, 1973 | Cow | Mesenteric vein, ex vivo | | 0.318 | Polarography |
| Pittman, 2005 | Rat | Mesenterial arteriolar wall | | 15 | Polarography |
| Tsai, 1998 | Rat | Mesenterial arteriolar wall, in vivo | | 390 | Phosphorescence quenching method |
| This study | Mouse | Dorsal skin window chamber arteriolar wall, in vivo | $6.0 \times 10^{-11}$ | 1.5 | Phosphorescence quenching method |

The cylinder tissue radius ($R$) for the arteriole, which is the distance between the arteriole center and the theoretical point of zero $pO_2$ gradient of the arteriolar wall, is necessary to calculate the oxygen consumption rate. The calculated value for $R$ was 56.3 ± 7.8 μm. To calculate the theoretical point of zero $pO_2$ gradient of the arteriolar wall, we used a curve-fitting technique on the measured $pO_2$ values at the three locations. The three measurement points were the intra-arteriolar, the wall center, and peri-arteriolar locations (**Fig. 3B**, gray plot) and these were assumed to represent values taken from the inner edge, wall center, and outer edge of the arteriolar wall (theoretical points; **Fig. 3B**, black plot), respectively. The calculated $R$ value indicated that oxygen molecules that diffuse through the arteriolar wall do not reach very far beyond the outer edge of arteriole.

## Discussion

### *Applicability of this method*

We made several assumptions to facilitate our study of the $K$ and $M$ values of the arteriolar wall. Mahler measured the oxygen diffusion constant using a strip of muscle tissue.[10] The tissue was placed

between two chambers; the upper chamber was insufflated with pure oxygen, and the oxygen concentration in the lower chamber was measured. The times from insufflation of pure oxygen in the upper chamber to the time when the oxygen concentration in the lower chamber started to increase and when it reached a stable level were measured

In our method, the animals were switched to inhalation of pure oxygen after breathing normal room air. There were several factors that influenced our measurements, including the several seconds that it took before the increase in blood oxygen tension was observed, according to the animal's condition, and the difference between the oxygen diffusion constants of the intravascular space (blood) and extravascular space (interstitial tissue). For these reasons, we could not use the same equations that Mahler had used.

We selected a method for directly measuring the time required for an oxygen molecule to go from inside the arteriolar lumen to the outer edge of the arteriole, defined as the diffusion time. If the diffusion velocity of the oxygen molecule in the arteriolar wall was slow enough to measure, we could use the formula for diffusion of small particles. This formula was first established by Einstein in 1905 using the formula for Brownian movement of molecules in a medium.[20] He gave the one-dimensional solution as $D = x^2/2t$. In this formula, $D$ represents the diffusion constant of the material, $x$ is distance, and $t$ is time. Because diffusion from the arteriole was defined two-dimensionally by Krogh, we used the two-dimensional formula $D = x^2/4t$, where $x$ represents the distance from the starting point of diffusion and $t$ is time. Using this formula, the oxygen diffusion constant of the arteriolar wall can be obtained when the thickness of the arteriolar wall and the time required for oxygen to reach

the outer arteriole wall is determined. We could measure the time required as the time when we observed a change in oxygen concentration at the outer arteriolar wall edge. Therefore, we used the formula for the diffusion constant given in Eq. 3.

Oxygen solubility ($\alpha$) of the arteriolar wall was defined according to Mahler.[10,11] Oxygen solubility of the arteriolar wall was determined using the change in oxygen tension (volume) at the outer edge of the arteriole and the inner edge of arteriolar wall (Eq. 4). Although the oxygen consumption rates of intra- and extra-arteriolar tissues differed, the patterns of $pO_2$ increase were similar (**Fig. 3A**). This phenomenon well supported our second measurement assumption that over a short period, the respective values of $M$ (oxygen consumption rate) for the tissue and arteriolar wall do not change.

The oxygen diffusion constant was measured using phosphorescence-quenching analysis. Pd-TCPP molecules in the excited triplet state in the laser irradiation area collided with oxygen molecules in the ground state. Oxygen molecules that were in an excited singlet state disappeared by reacting with nearby molecules. Consequently, $pO_2$ recovered because of the diffusion of nearby oxygen. However, to measure the oxygen diffusion constant, a laser must be used for the irradiation pulse interval before the oxygen diffusion phenomenon in tissue in order to detect the velocity of oxygen movement. The inner and outer edges of the arteriolar wall were chosen as the laser irradiation points. We predicted that the oxygen diffusion constants of the intra-arteriolar bloodstream and peri-arteriolar tissue areas would be higher than those of the arteriolar wall. The diffusion time of oxygen in the arteriolar wall was measurable; this fact suggests that the oxygen diffusion constant of the arteriolar wall is lower than that in the surrounding tissue, indicating that our third assumption is valid. Furthermore, the $pO_2$ of laser-irradiated spots located beside the arteriolar wall did not decrease during measurement. Each spot was laser-excited with a 5-Hz frequency, which suggests that the oxygen consumption resulting from Pd-TCPP phosphorescence emission was very low and that the power and time interval of the pulse laser irradiation were appropriate.

We used a 23-μm-diameter laser beam to measure oxygen tension by the phosphorescence-quenching method. The laser beam diameter could have been smaller, but a smaller diameter would cause larger deviations because of the variety of cell types in the tissue. Pulsatile movement of the arteriolar wall might also contribute to such fluctuations. Moreover, if we had used a smaller diameter laser beam, to detect the appropriate strength of phosphorescence, a stronger laser power would have been necessary and this might have damaged the tissue. Therefore, to detect stable average levels of tissue oxygen tension semi-continuously without tissue damage, we used a 23-μm-diameter laser beam at the focus position.

### *Comparison of oxygen diffusion from the arteriolar wall and oxygen consumption in the arteriolar wall*

The amount of oxygen diffusion ($Q_K$) and oxygen consumption ($Q_M$) in the arteriolar wall were compared. When a 100-μm length of arteriole is considered,[6] the oxygen diffusion and oxygen consumption can be calculated from $K$ and $M$ values for the arteriolar wall using Eqs. 9 and 10:

$$Q_K = K \cdot \frac{\partial pO_2}{\partial r} \cdot S \tag{9}$$

$$Q_M = M \cdot V_t \tag{10}$$

where $S$ is the inner surface area of the arteriolar wall, $V_t$ is the volume of the arteriolar wall, and $\partial pO_2/\partial r$ is the $pO_2$ gradient in the arteriolar wall.

The calculated $Q_K$ was $1.4 \times 10^{-10}$ (ml·s$^{-1}$·100 μm$^{-1}$ arteriole length), and $Q_M$ was $1.2 \times 10^{-10}$ (ml·s$^{-1}$·100 μm$^{-1}$ arteriole length) (**Table 1**). These data suggest that the oxygen that diffused from the lumen of the arteriole was absorbed into or consumed by the arteriolar wall. The structure of the arteriolar wall is simpler than that of the aorta and arteries in general; the oxygen diffusion constant of the arteriolar wall is considered to be higher than that of either the aorta or artery walls. Smooth muscle cells in the arteriolar wall require an abundant oxygen supply. We used a laser-evoked phosphorescence decay assay to evaluate the tissue oxygen tension. Because the $pO_2$ gradient adjacent to the arteriolar wall was considered to be steep, the $pO_2$ of the tissue obtained by our system might be lower than the true value. If this is the case, then the true $M$ value might be lower than the calculated value we obtained from the experimental data.

### *Oxygen balance (consumption and diffusion)*

In the downstream direction, $pO_2$ in arterioles has been found to decrease by 2–3% per 100 μm.[28] We calculated the oxygen loss ($Q$) for a 100 μm length of arteriole as follows:

$$Q = V_b \cdot \frac{\partial P_{lose}}{2\partial z} \cdot (L \cdot v^{-1})^{-1} \tag{11}$$

where $V_b$ is the blood volume, $\partial P_{lose}/\partial z$ is the oxygen loss rate per 100 μm of arteriole, $L$ is the length (a 100 μm in this case), and $v$ is the red blood cell velocity.

The $pO_2$ loss rate per 100 μm of arteriole was calculated as 4.5%±1.3% ($N = 4$). We also measured the RBC velocity and $pO_2$ and calculated the oxygen balance. Calculations were conducted using the experimental data presented in **Table 1**; the mean RBC velocity for the whole arteriole was calculated based on the average velocity at

the center of the vessel (2.80 ± 1.31 mm/s) following the Baker–Wayland model.[24]

The calculated oxygen loss, $Q$, of 1.8 ± 0.5 × $10^{-10}$ (ml·$s^{-1}$·100 μ$m^{-1}$ arteriole length) was very similar to the amount of oxygen diffusion, $Q_K$, [1.4 × $10^{-10}$(ml·$s^{-1}$·100 μ$m^{-1}$ arteriole length)], demonstrating that the value of $K$ of the arteriolar wall was lower than that of the other tissues. Our study showed that the oxygen diffusion constant $K$ of arteriolar wall was 6.0 ± 1.2 × $10^{-11}$ [($cm^2$/s)(ml $O_2$·$cm^{-3}$ tissue·$mmHg^{-1}$)], which was one-tenth the value for hamster retractor muscle reported by Bentley.[1] Muscle is tissue that consumes oxygen to function, whereas arterioles comprise tissue conveying oxygen and nutrients. A high oxygen diffusion constant in muscle tissue and low oxygen diffusion constant in the arteriolar wall seems rational for maintaining the oxygen balance. Previous reports have presented various values for the oxygen consumption rate (**Table 2**). The values of $M$ listed on **Table 2** are close to 1 (ml $O_2$·100 $cm^{-3}$ tissue·$min^{-1}$), except for the value of 390 (ml $O_2$·100 $cm^{-3}$ tissue·$min^{-1}$) reported by Tsai et al.[6] Thus, our results confirmed what many investigators have reported over the past 40 years. The high value reported by Pittman was calculated using the arrested flow method.[26] We believe that they reported the maximum value for wall consumption by assuming that all of the oxygen disappeared from the arteriolar lumen, thereby setting an upper limit on $M$. Differences in the values of various reports might result from differences in the targeted tissues or measurement methods. Because the arteriolar wall comprises various cell types (endothelium, smooth muscle cells, and pericytes) and matrices (basement membrane, collagen, and elastin), the results show that the vessel wall functions partly as a barrier to oxygen and partly as a permeable membrane.

### *Applicability of the results of this study*

Because we measured the $K$ of arteriolar wall, we were able to assess the applicability of therapeutic approaches that change the value of $K$. For example, if the experiment were to be conducted in a hyperbaric oxygen chamber or after administration of certain drugs that alter arteriolar wall characteristics, the efficacy could be investigated. In light of the oxygen cascade, the arteriole is inevitably in an upstream location. We would be able to increase the oxygen supply of capillaries and venules if we could reduce the value of arteriolar $K$ or $M$, thereby producing an oxygen-rich environment for peripheral tissues. Such arteriolar wall modifications might be useful for improving the function of ischemic organs or altering tumor growth.

## Acknowledgments

The authors are grateful to Prof. Marcos Intaglietta (Department of Bioengineering, University of California, La Jolla, California) for discussions and valuable advice. This study was supported in part by a Grant-in-Aid for Scientific Research (H.H. No. C-21591824) from the Ministry of Education, Culture, Sports, Science and Technology of Japan.

## References

1. Krogh A: The number and distribution of capillaries in muscles with calculations of the oxygen pressure head necessary for supplying the tissue. J Physiol 1919; **52**: 409–415. [Medline]
2. Krogh A: The supply of oxygen to the tissues and the regulation of the capillary circulation. J Physiol 1919; **52**: 457–474. [Medline]
3. Swain DP, Pittman RN: Oxygen exchange in the microcirculation of hamster retractor muscle. Am J Physiol 1989; **256**: H247–H255. [Medline]
4. Honig CR, Gayeski TE, Clark A Jr, Clark PA: Arteriovenous oxygen diffusion shunt is negligible in resting and working gracilis muscles. Am J Physiol 1991; **261**: 2031–2043. [Medline]
5. Sharan M, Vovenko EP, Vadapalli A, Popel AS, Pittman RN: Experimental and theoretical studies of oxygen gradients in rat pial microvessels. J Cereb Blood Flow Metab 2008; **28**: 1597–1604. [Medline] [CrossRef]
6. Tsai AG, Friesenecker B, Mazzoni MC, Merger H, Buerk DG, Johnson PC, Intaglietta M: Microvascular and tissue oxygen gradients in the rat mesentery. Proc Natl Acad Sci USA 1998; **95**: 6590–6595. [Medline] [CrossRef]
7. Vovenko EP: Transmural oxygen tension gradients in rat cerebral cortex arterioles. Neurosci Behav Physiol 2009; **39**: 363–370. [Medline] [CrossRef]
8. Bergers G, Song S: The role of pericytes in blood-vessel formation and maintenance. Neuro-oncology 2005; **7**: 452–464. [Medline] [CrossRef]
9. Shibata M, Ichioka S, Kamiya A: Estimating oxygen consumption rates of arteriolar walls under physiological conditions in rat skeletal muscle. Am J Physiol Heart Circ Physiol 2005; **289**: 295–300. [Medline] [CrossRef]
10. Mahler M: Diffusion and consumption of oxygen in the resting frog sartorius muscle. J Gen Physiol 1978; **71**: 533–557. [Medline] [CrossRef]
11. Mahler M, Louy C, Homsher E, Peskoff A: Reappraisal of diffusion, solubility, and consumption of oxygen in frog skeletal muscle, with applications to muscle energy balance. J Gen Physiol 1985; **86**: 105–134. [Medline] [CrossRef]
12. Mueller-Klieser W: Method for the determination of oxygen consumption rates and diffusion coefficients in multicellular spheroids. Biophys J 1984; **46**: 343–348. [Medline] [CrossRef]
13. Ushiyama A, Yamada S, Ohkubo C: Microcirculatory parameters measured in subcutaneous tissue of the mouse using a novel dorsal skinfold chamber. Microvasc Res 2004; **68**: 147–152. [Medline] [CrossRef]
14. Shibata M, Ichioka S, Ando J, Kamiya A: Microvascular and interstitial PO(2) measurements in rat skeletal muscle by phosphorescence quenching. J Appl Physiol 2001; **91**: 321–327. [Medline]
15. Torres Filho IP, Leunig M, Yuan F, Intaglietta M, Jain RK: Noninvasive measurement of microvascular and interstitial oxygen profiles in a human tumor in SCID mice. Proc Natl Acad Sci USA 1994; **91**: 2081–2085. [Medline] [CrossRef]
16. Tsukada K, Sekizuka E, Oshio C, Tsujioka K, Minamitani H: Red blood cell velocity and oxygen tension measurement in cerebral microvessels by double-wavelength photoexcitation. J Appl Physiol 2004; **96**: 1561–1568. [Medline] [CrossRef]
17. Sinaasappel M, Ince C: Calibration of Pd-porphyrin phosphorescence for oxygen concentration measurements in vivo. J Appl Physiol 1996; **81**: 2297–2303. [Medline]

18. Bentley TB, Meng H, Pittman RN: Temperature dependence of oxygen diffusion and consumption in mammalian striated muscle. Am J Physiol 1993; **264**: H1825–H1830. [Medline]
19. Edidin M, Fambrough D: Fluidity of the surface of cultured muscle fibers. Rapid lateral diffusion of marked surface antigens. J Cell Biol 1973; **57**: 27–37. [Medline] [CrossRef]
20. Einstein A: On the movement of small particles suspended in stationary liquids required by the molecular-kinetic theory of heat. Annalen Phys 1905; **17**: 549–560. [CrossRef]
21. Yano Y, Sato K: Oxygen diffusion introductory book. Environmental Research and Control Center, Ltd., 1978; 52–156. [in Japanese].
22. Ogi T: Rika Nenpyo. National Astronomical Observatory of Japan. Maruzen Co. Ltd., 2010; 503.
23. Madsen J, Trefny J: Transient heat pulse technique for low thermal diffusivity solids. J Phys E Sci Instrum 1988; **21**: 363–366. [CrossRef]
24. McGuire BJ, Secomb TW: A theoretical model for oxygen transport in skeletal muscle under conditions of high oxygen demand. J Appl Physiol 2001; **91**: 2255–2265. [Medline]
25. Pittman RN, Ellsworth ML: Estimation of red cell flow in microvessels: consequences of the Baker–Wayland spatial averaging model. Microvasc Res 1986; **32**: 371–388. [Medline] [CrossRef]
26. Pittman RN, Golub AS, Schleicher WF: Rate of decrease of PO2 from an arteriole with arrested flow. Adv Exp Med Biol 2005; **566**: 257–262. [Medline] [CrossRef]
27. Buerk DG, Goldstick TK: Arterial wall oxygen consumption rate varies spatially. Am J Physiol 1982; **243**: H948–H958. [Medline]
28. Howard RO, Richardson DW, Smith MH, Patterson JL Jr: Oxygen consumption of arterioles and venules as studied in the Cartesian diver. Circ Res 1965; **16**: 187–196. [Medline]
29. Navari RM, Wei EP, Kontos HA, Patterson JL Jr: Oxygen consumption of pial arteries. Am J Physiol 1979; **236**: H151–H156. [Medline]
30. Paul RJ, Peterson JW, Caplan SR: Oxygen consumption rate in vascular smooth muscle: relation to isometric tension. Biochim Biophys Acta 1973; **305**: 474–480. [Medline] [CrossRef]